Journal of Geriatric Cardiology (2015) 12: 410–416

Research Article · Open Access ·

Liraglutide reduces oxidized LDL-induced oxidative stress and fatty degeneration in Raw 264.7 cells involving the AMPK/SREBP1 pathway

Yan-Gui WANG[1,2], Tian-Lun YANG[1]

[1]*Department of Cardiology, Xiangya Hospital, Central South University, No. 87 Xiangya Road, Changsha, Hunan, China*
[2]*Deparment of Geriatrics, Hunan Provincial People's Hospital, No.61 Jiefang West Road, Changsha, Hunan, China*

Abstract

Backgound Recent studies have suggested a potential role for liraglutide in the prevention and stabilization of atherosclerotic vascular disease. However, the molecular mechanisms underlying the effect of liraglutide on atherosclerosis have not been well elucidated. The purpose of this study was to examine whether liraglutide protects against oxidative stress and fatty degeneration *via* modulation of AMP-activated protein kinase (AMPK)/sterol regulatory element binding transcription factor 1 (SREBP1) signaling pathway in foam cells. **Methods** Mouse macrophages Raw264.7 cells were exposed to oxidized low density lipoprotein (oxLDL) to induce the formation of foam cells. The cells were incubated with oxLDL (50 μg/mL), liraglutide (0.1, 0.5, 1 and 2 nmol/L) or exendin-3 (9-39) (1, 10 and 100 nmol/L) alone, or in combination. Oil Red O staining was used to detect intracellular lipid droplets. The levels of TG and cholesterol were measured using the commercial kits. Oxidative stress was determined by measuring intracellular reactive oxygen species (ROS), malondialdehyde (MDA) and superoxide dismutase 1 (SOD). Western blot analysis was used to examine the expression of AMPKα1, SREBP1, phosphorylated AMPKα1, phosphorylated SREBP1, glucagon-like peptide-1 (GLP-1) and GLP-1 receptor (GLP-1R). **Results** Oil Red O staining showed that the cytoplasmic lipid droplet accumulation was visibly decreased in foam cells by treatment with liraglutide. The TG and cholesterol content in the liraglutide-treated foam cells was significantly decreased. In addition, foam cells manifested an impaired oxidative stress following liraglutide treatment, as evidenced by increased SOD, and decreased ROS and MDA. However, these effects of liraglutide on foam cells were attenuated by the use of GLP-1R antagonist exendin-3 (9-39). Furthermore, we found that the expression level of AMPKα1 and phosphorylated AMPKα1 was significantly increased while the expression level of SREBP1 and phosphorylated SREBP1 was significantly decreased in foam cells following treatment with liraglutide. **Conclusions** This study for the first time demonstrated that the effect of liraglutide on reducing oxidative stress and fatty degeneration in oxLDL-induced Raw264.7 cells is accompanied by the alteration of AMPK/SREBP1 pathway. This study provided a potential molecular mechanism for the effect of liraglutide on reducing oxidative stress and fatty degeneration.

J Geriatr Cardiol 2015; 12: 410–416. doi:10.11909/j.issn.1671-5411.2015.04.013

Keywords: AMPK/SREBP1 pathway; Fatty degeneration; Foam cell; Liraglutide; Oxidative stress

1 Introduction

Atherosclerosis is the most common pathological process underlying cardiovascular diseases (CVD). It is a disease of the large- and medium-size arteries that is characterized by a formation of atherosclerotic plaques.[1–3]

Liraglutide, a glucagon-like peptide-1 (GLP-1) analogue with 97% homology to native GLP-1, increases insulin secretion and insulin sensitivity.[4] Recent studies have suggested a potential role for liraglutide in the prevention and stabilization of atherosclerotic vascular disease together with possible protection against major cardiovascular events.[5]

AMP-activated protein kinase (AMPK) is a major regulator of glucose and lipid metabolism.[6] It has been reported that AMPK activation attenuates oxidized low density lipoprotein (oxLDL)-induced lipid accumulation in murine macrophages and promotes cholesterol efflux from lipid-laden cells.[7] Until now, relatively few studies have investigated whether liraglutide could reduce lipid accumulation through modulating the AMPK/sterol regulatory element binding transcription factor 1 (SREBP1) pathway.

Foam cells are the characteristic pathological cells in atherosclerotic plaques.[8] In the present study, a macrophage-derived foam cell model was established, and we

Correspondence to: Tian-Lun YANG, PhD, Department of Cardiology, Xiangya Hospital, Central South University, No. 87 Xiangya Road, Changsha, Hunan, China. E-mail: tlyang135@163.com
Telephone: +86-731-84327250 **Fax:** +86-731-84327250
Received: January 31, 2015 **Revised:** March 23, 2015
Accepted: May 6, 2015 **Published online:** July 3, 2015

examined whether the AMPK/SREBP1 pathway was involved in the effect of liraglutide on reducing oxidative stress and fatty degeneration in foam cells.

2 Methods

2.1 Cell culture

Raw264.7 macrophages were purchased from the American Type Culture Collection (ATCC; Manassas, VA, USA). The cells were cultured in Dulbecco's modified Eagle's medium (Gibco-BRL, Grand Island, NY, USA) supplemented with 10% fetal bovine serum (Gbico-BRL) in a humidified 37°C incubator with 5% CO_2. OxLDL was obtained from DingGuo Biotech (Chongqing, China), liraglutide was provided by Novo Nordisk (Copenhagen, Denmark) and exendin-3 (9-39) was purchased from Santa Cruz Biotechnology, Inc. (Santa Cruz, CA, USA). The cells were incubated with oxLDL (50 μg/mL), liraglutide (0.1, 0.5, 1 and 2 nmol/L) or exendin-3 (9-39) (1, 10 and 100 nM) alone, or in combination.

2.2 Oil Red O staining

For Oil Red O staining, the cells were fixed with 10% formaldehyde for 10 min. After washing with phosphate-buffered saline (PBS), the cells were stained with filtered Oil Red O solution (60% Oil Red O dye and 40% water) (Sigma-Aldrich, St. Louis, MO, USA) at room temperature (r.t) for 15 min. The cells were then washed with PBS to remove unbound dye and observed under the microscope (TE200; Nikon, Tokyo, Japan).

2.3 Measurement of triglyceride and total cholesterol

The triglyceride (TG) level was determined in cell lysates using a Triglyceride Quantification Kit (Abcam, Cambridge, MA, USA) according to the manufacturer's instructions. Briefly, a standard curve was prepared with the TG Stand. The cells were homogenized in 5% NP-40 and heated at 80-100°C for 2-5 min. After centrifugation, 2 μL of lipase was added to each standard and sample well, and incubated at room temperature for 20 min. A total 50 μL reaction mix, containing 46 μL Triglyceride Assay Buffer, 2 μL Triglyceride Probe and 2 μL Triglyceride Enzyme Mix, was added to each well and incubated at r.t. for 30-60 min. The optical density at 570 nm was measured in a microtiter plate reader (ELx800NB; BioTek Instruments, Inc., Winooski, VT, USA).

The level of total cholesterol (TC) in cells was determined using a Cholesterol Assay Kit from Abcam (Cambridge, MA, USA) following the manufacturer's instructions. Briefly, the standard curve was prepared using 2 μg/μL cholesterol Standard and the cells were lysed by ultrasonic wave. The cells were then frozen and thawed three times. After centrifugation at 4°C for 10 min, the supernatant was collected. A total 50 μL Reaction Mix containing 44 μL Cholesterol Assay Buffer, 2 μL Cholesterol Probe, 2 μL Enzyme Mix and 2 μL Cholesterol Esterase was prepared and added to each well. The plates were incubated at 37°C for 60 min. The optical density at 570 nm was measured in a microtiter plate reader (ELx800NB; BioTek Instruments, Inc.).

2.4 Measurement of intracellular reactive oxygen species production, malondialdehyde and superoxide dismutase

The Reactive Oxygen Species (ROS) Assay Kit was purchased from Beyotime (Shanghai, China). After washing with PBS, the cells were suspended in the DCFH-DA solution (10 μmol/L) at a final density of 10^7 cells/mL and incubated at 37°C for 20 min. Fluorescent intensity was measured by a fluorospectrophotometer (F-4000; Hitachi, Ltd., Tokyo, Japan).

The cells were sonicated in 0.1 mol/L Tris-HCl buffer (pH 7.4) containing 0.5% Triton X-100, 5 mmol/L β-mercaptoethanol and 0.1 mg/mL phenylmethylsulfonyl fluoride. The homogenates were centrifuged at 1,000 r/min at 4°C for 5 min, and the supernatants were used for measuring cellular malondialdehyde (MDA) and superoxide dismutase (SOD). MDA was determined using the thiobarbituric acid (TBA) method. The level of MDA was measured using a Lipid Peroxidation MDA Assay Kit (Beyotime) according to the instructions of the manufacturer. The thiobarbituric acid reacting substances at a wavelength of 532 nm was determined using the EL× 800NB microplate reader (Bio-Tek Instruments, Inc.). The MDA level is expressed as μmol/mg protein. SOD activity was examined by the xanthine oxidase method using a Superoxide Dismutase Activity Assay Kit (BioVision, Milpitas, CA, USA). The absorbance was determined at 450 nm using a microplate reader (ELx800NB; BioTek Instruments, Inc.).

2.5 Western blot analysis

The primary antibodies, including rabbit monoclonal to AMPK alpha 1, rabbit polyclonal to AMPK alpha 1 (phospho S487), rabbit monoclonal to AMPK alpha 1 (phospho S496), rabbit polyclonal to SREBP1, rabbit polyclonal to SREBP1 (phospho S372) and rabbit polyclonal to SREBP1 (phospho S439) were purchased from Abcam. The primary antibodies, including mouse monoclonal to GLP-1, mouse monoclonal to GLP-1R, mouse monoclonal to β-actin, and the secondary antibodies (goat anti rabbit IgG/HRP and goat anti mouse IgG/HRP) were obtained from Santa Cruz.

The cells were lysed in RIPA buffer (Sangon Biotech,

Shanghai, China) and protein concentrations were quantified by the BCA method using the BCA Protein Assay Kit (Beyotime). A total of 0.50 mg of protein was separated by 12% SDS polyacrylamide gel and transferred onto polyvinylidene difluoride membranes (Millipore, Billerica, MA, USA). The membranes were blocked via incubation with tris-buffered saline containing 5% non-fat milk at 37°C for 2 h. Thereafter, the membranes were incubated with the primary antibodies at 37°C for 1 h. Bands were detected by horseradish peroxidase-coupled secondary antibody and chemiluminescence (ECL Western blotting kit; Pierce, Rockford, IL, USA).

2.6 Statistical analyses

SPSS 19.0 (IBM Corporation, Armonk, NY, USA) was used for statistical analyses. Data were expressed as the mean ± SD. The difference between the two groups was evaluated using the Student's *t*-test. $P < 0.05$ was considered to indicate a statistically significant difference.

3 Results

3.1 OxLDL induced foam cell formation in Raw264.7 cells

To establish the macrophage-derived foam cell model, Raw264.7 macrophages were incubated with 50 μg/mL oxLDL for 48 h. It was shown in Figure 1 that oxLDL induced the foam cell formation; the cytoplasmic lipid droplet accumulation was visibly increased in Raw274.7 following oxLDL treatment.

3.2 Liraglutide activated AMPK/SREBP1 pathway in oxLDL-stimulated Raw264.7 cells

To investigate the effect of liraglutide on the AMPK/SREBP1 pathway in macrophage-derived foam cells, Raw264.7 cells were exposed to oxLDL (50 μg/mL) in the absence or presence of liraglutide (0.1, 0.5, 1 and 2 nmol/L) for 48 h. Treatment with 50 μg/mL oxLDL for 48 h resulted in a decrease in the amount of AMPKα1 (0.234 ± 0.051 *vs.* 0.074 ± 0.015, $P < 0.01$), pho-AMPKα1 (S487) (0.158 ± 0.031 *vs.* 0.060 ± 0.012, $P < 0.01$) and pho-AMPKα1 (S496) (0.136 ± 0.032 *vs.* 0.038 ± 0.008, $P < 0.01$) in Raw264.7 cells. A significant increase of SREBP1 was observed in Raw264.7 cells treated with oxLDL (0.014 ± 0.004 *vs.* 0.141 ± 0.037, $P < 0.01$). In addition, we found that oxLDL shows inhibitory effect on the expression of GLP-1 (0.212 ± 0.048 *vs*. 0.122 ± 0.027, $P < 0.05$) and GLP-1R (0.324 ± 0.054 *vs*. 0.188 ± 0.039, $P < 0.05$).

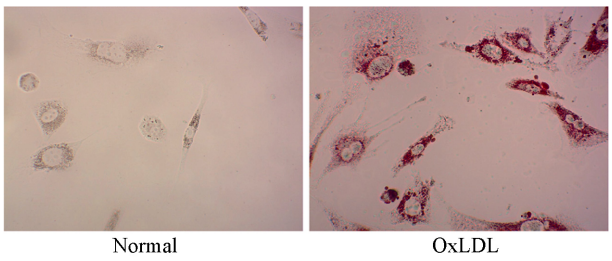

Figure 1. Oil Red O staining of Raw264.7 cells exposed to oxLDL. × 400. OxLDL: oxidized low density lipoprotein.

It was shown in Figure 2 that 0.5 nmol/L to 2 nnmol/L liraglutide significantly increased the expression of AMPKα1, pho-AMPKα1 (S487) and pho-AMPKα1 (S496) with the peak value at 1 nmol/L. The expression of SREBP1 was markedly decreased by treatment with liraglutide at the concentrations of 1 nmol/L and 2 nmol/L (Figure 3).

Next, 1 nmol/L liraglutide was added to treat oxLDL-stimulated Raw264.7 cells together with excendin-3 (9-39), a potent and selective GLP-1 receptor (GLP-1R)

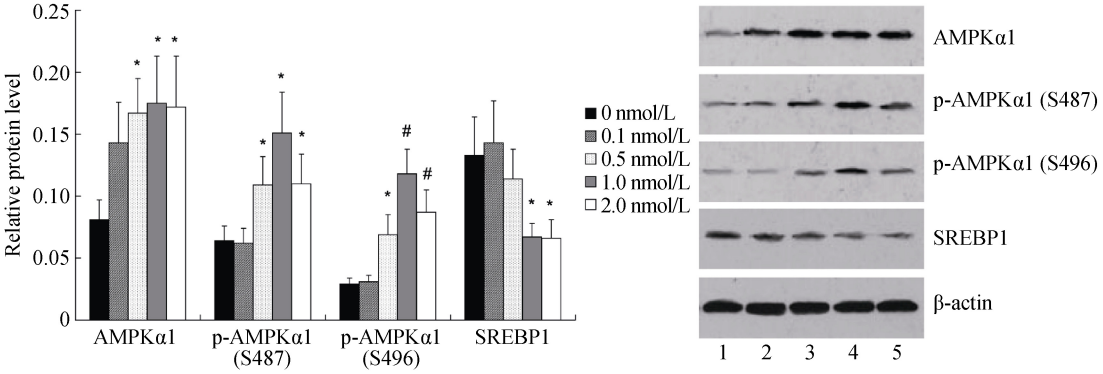

Figure 2. Effect of liraglutide on AMPK/SREBP1 pathway in oxLDL-stimulated Raw264.7 cells. *$P < 0.05$, **$P < 0.01$ *vs*. 0 nmol/L group. OxLDL-stimulated Raw264.7 cells were treated with liraglutide at the concentration of 0.1, 0.5, 1 and 2 nmol/L. The expression of AMPKα1, phospho- AMPKα1 and SREBP1 was determined by western blot analysis. β-actin expression was used as an internal control. Lane 1, 0 nmol/L; lane 2, 0.1 nmol/L; lane 3, 0.5 nmol/L; lane 4, 1 nmol/L; lane 5, 2 nmol/L. OxLDL: oxidized low density lipoprotein; p-AMPKα1: phosphorylated AMP-activated protein kinase alpha 1; SREBP1: sterol regulatory element binding transcription factor 1.

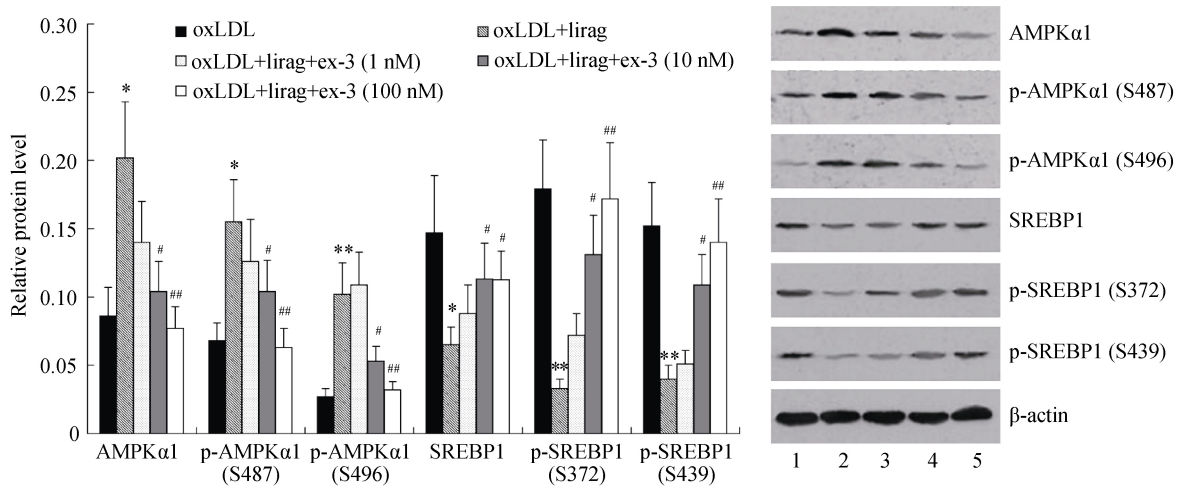

Figure 3. Exendin-3 (9-39) attenuated effect of liraglutide on AMPK/SREBP1 pathway in oxLDL-stimulated Raw264.7 cells. *P < 0.05, **P < 0.01 *vs*. oxLDL group; $^{\#}P$ < 0.05, $^{\#\#}P$ < 0.01 *vs*. oxLDL+lirag group. OxLDL-stimulated Raw264.7 cells were incubated with liraglutide (1 nmol/L) and exendin-3 (9-39) at the concentration of 1, 10 and 100 nmol/L. The expression of AMPKα1, phospho-AMPKα1, SREBP1 and phospho-SREBP1 was determined by western blot analysis. β-actin expression was used as an internal control. Lane 1, oxLDL group; lane 2, oxLDL+lirag group; lane 3, oxLDL+lirag+ex-3 (1 nmol/L) group; lane 4, oxLDL+lirag+ex-3 (10 nmol/L); lane 5, oxLDL+lirag+ex-3 (100 nmol/L) group. Ex-3: exendin-3 (9-39); lirag: liraglutide; oxLDL: oxidized low density lipoprotein; p-AMPKα1: phosphorylated AMP-activated protein kinase alpha 1; p-SREBP1: phosphorylated sterol regulatory element binding transcription factor 1.

antagonist, at concentrations of 1 nmol/L, 10 nmol/L and 100 nmol/L. As shown in Figure 3, we found that compared with the liraglutide group, the expression of AMPKα1, pho-AMPKα1 (S487) and pho-AMPKα1 (S496) was significantly decreased, while the expression of SREBP1, pho-SREBP1 (S372) and pho-SREBP1 (S439) was significantly increased in the liraglutide+10 nmol/L excendin-3 group and liraglutide+100 nmol/L excendin-3 group.

3.3 Liraglutide suppressed oxLDL-induced foam cell formation and lipid accumulation in Raw264.7 cells

To determine the effect of liraglutide on oxLDL-induced foam cell formation, Raw 264.7 cells were exposed to oxLDL (50 μg/mL) in the presence, or absence of liraglutide (1 nmol/L) for 48 h, Oil Red O staining was then performed. The pictures of Oil Red O staining were shown in Figure 4.

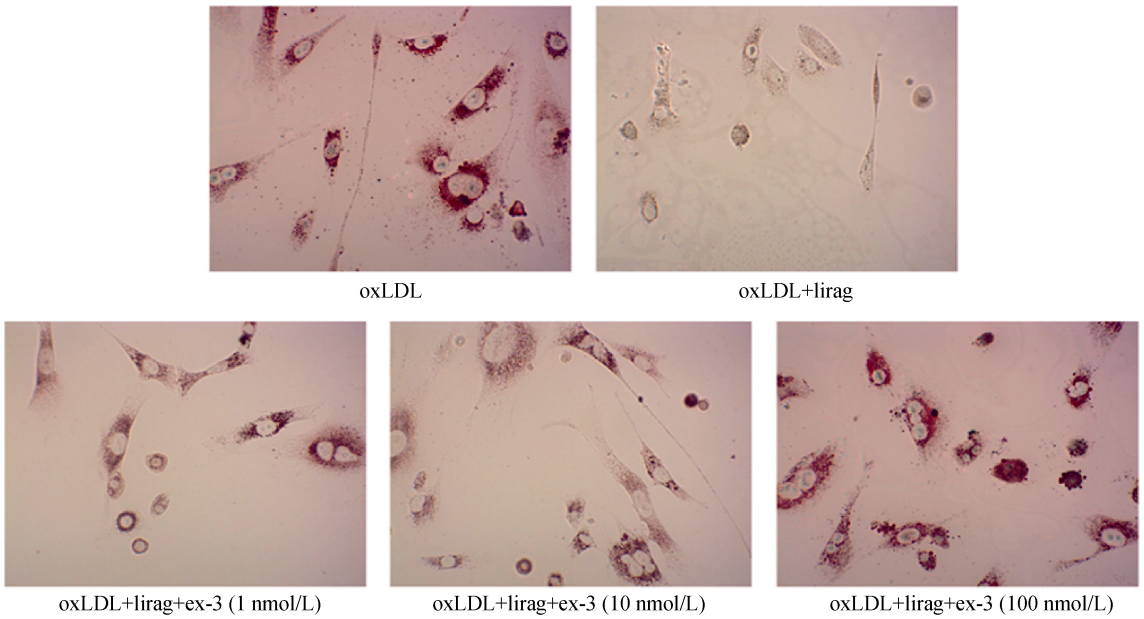

Figure 4. Liraglutide suppressed oxLDL-induced foam cell formation in Raw264.7 cells. Oil Red O staining of oxLDL-stimulated Raw264.7 cells following incubation with liraglutide (1 nmol/L) and exendin-3 (9-39) (1, 10 and 100 nmol/L). Magnification, × 400. Ex-3: exendin-3 (9-39); lirag: liraglutide; oxLDL: oxidized low density lipoprotein.

It was revealed that the cytoplasmic lipid droplet accumulation was visibly decreased by treatment with liraglutide (1 nmol/L). When oxLDL-stimulated Raw264.7 cells were treated with excendin-3 (1-100 nmol/L) and liraglutide (1 nmol/L), the cytoplasmic lipid droplet accumulation was increased with excendin-3 in a dose-dependent manner. Furthermore, we found that the levels of TG and TC were significantly increased in Raw264.7 cells treated with 50 μg/mL oxLDL. Liraglutide (1 nmol/L) inhibited the elevated levels of TG and TC in oxLDL-stimulated Raw264.7 cells. However, this effect was attenuated by excendin-3 (9-39). The levels of TG and TC were significantly increased when oxLDL-stimulated Raw264.7 cells were treated with 10 nmol/L and 100 nmol/L excendin-3 (9-39) (Figure 5).

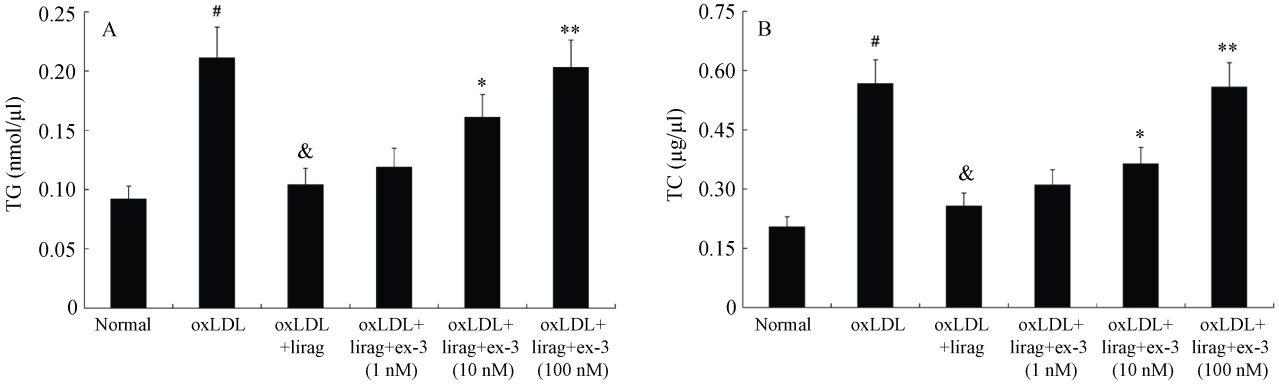

Figure 5. Liraglutide suppressed oxLDL-induced fatty degeneration in Raw264.7 cells. (A) The level of TG in oxLDL-stimulated Raw264.7 cells following incubation with liraglutide (1 nmol/L) and exendin-3 (9-39) (1,10 and 100 nmol/L). (B) The level of TC in oxLDL-stimulated Raw264.7 cells following incubation with liraglutide (1 nmol/L) and exendin-3 (9-39) (1, 10 and 100 nmol/L). $^{\#}P < 0.01$ *vs*. normal group, $^{\&}P < 0.01$ *vs*. oxLDL group, $^{*}P < 0.05$, $^{**}P < 0.01$ *vs*. oxLDL+lirag group. Ex-3: exendin-3 (9-39); lirag: liraglutide; oxLDL: oxidized low density lipoprotein; TC: total cholesterol; TG: triglyceride.

3.4 Liraglutide suppressed oxLDL-induced oxidative stress in Raw264.7 cells

As shown in Figure 6, incubation of Raw264.7 cells with 50 μg/mL oxLDL for 48 h resulted in a significant increase of ROS production and MDA, but a significant decrease of SOD.

Co-treatment with oxLDL and liraglutide (1nmol/L) inhibited oxLDL induced ROS and MDA. In the meanwhile, the expression of SOD was significantly increased when oxLDL-stimulated Raw264.7 cells were treated with liraglutide (1 nmol/L).

Compared with the liraglutide group, oxLDL-stimulated Raw264.7 cells-treated with excendin-3 (1-100 nmol/L) showed an increased ROS and MDA, but a decreased SOD in a dose-dependent manner.

4 Discussion

Foam cells, which are mainly derived from blood macrophages and vascular smooth muscle cells, appear to be the characteristic pathological cells in atherosclerotic plaques.[8] During the process of atherosclerosis, mononuclear cells recruit to the intima of the artery, and transform into macrophages.[9] Uptake of modified forms of LDL by the macrophages through scavenger receptors [10–13] will lead to the formation of foam cells.[14–17] It is well documented that the uptake of oxLDL by the macrophage will induce foam cell formation and promote the development of atherosclerosis.[18–22] In the present study, we established the *in vitro* macrophage derived foam cell model by exposing mouse macrophages Raw264.7 cells to 50 μg/mL oxLDL for 48 h for studies on atherosclerosis.

Liraglutide was previously used for the treatment of diabetes.[4] Recently, some *in vivo* studies have revealed the potential function of liraglutde in improving non-alcoholic fatty liver disease (NAFLD) and atherosclerotic vascular disease.[5,23,24] However, there is no *in vitro* report about the effect of liraglutide on foam cells until now. Increasing evidence shows that oxidative stress plays an important role in the pathogenesis of atherosclerosis.[25] Oxidative stress is defined as an imbalanced redox state in which pro-oxidants overwhelm antioxidant capacity, resulting in an increased ROS production. SOD is an important antioxidant enzyme which converts naturally- occurring, but harmful superoxide radicals to molecular oxygen and hydrogen peroxide. MDA, a secondary oxidation product formed during the oxidation of polyunsaturated fatty acids (PUFA), is frequently used as an index of lipid peroxidation. In the present study, we firstly investigated the effect of liraglutide on oxidative stress and fatty degeneration in foam cells. Consistent with the results obtained from a recent study on NAFLD,[24] we revealed a potential novel role of liraglutide in improving oxidative stress and lipid accumulation in the macrophage-derived foam cell model. The inhibitory effect of liraglutide on oxLDL-induced lipid accumulation and oxidative stress

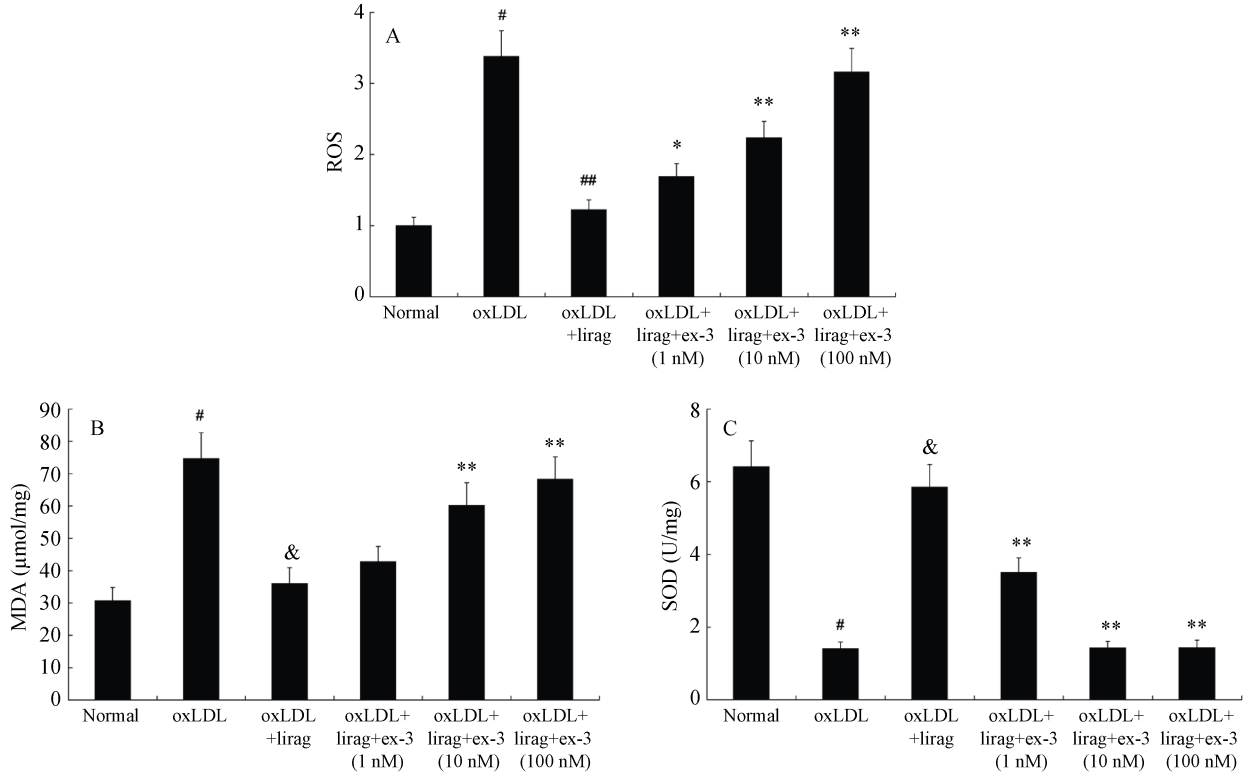

Figure 6. Liraglutide suppressed oxLDL-induced oxidative stress in Raw264.7 cells. (A) The ROS production in oxLDL-stimulated Raw264.7 cells following incubation with liraglutide (1 nmol/L) and exendin-3 (9-39) (1, 10 and 100 nmol/L). (B) The level of MDA in oxLDL-stimulated Raw264.7 cells following incubation with liraglutide (1 nmol/L) and exendin-3 (9-39) (1,10 and 100 nmol/L). (C) The level of SOD in oxLDL-stimulated Raw264.7 cells following incubation with liraglutide (1 nmol/L) and exendin-3 (9-39) (1, 10 and 100 nmol/L). $^{\#}P < 0.01$ *vs*. normal group, $^{\&}P < 0.01$ *vs*. oxLDL group, $^{*}P < 0.05$, $^{**}P < 0.01$ *vs*. oxLDL+lirag group. Ex-3: exendin-3 (9-39); lirag: liraglutide; MDA: malondialdehyde; oxLDL: oxidized low density lipoprotein; ROS: reactive oxygen species; SOD: superoxide dismutase.

was attenuated by the selective GLP-1R antagonist exendin-3 (9-39), it demonstrated that this effect is dependent on GLP-1R.

AMPK is a phylogenetically conserved serine/threonine kinase that mediates cellular energy homeostasis.[26, 27] When activated, AMPK triggers a switch from ATP-consuming anabolic pathways to ATP-producing catabolic pathways. AMPK activation is associated with the inhibition of TG and cholesterol synthesis, lipogenesis, and the stimulation of hepatic fatty acid oxidation.[28, 29] AMPK negatively regulates several proteins central to the lipid metabolism process, such as PPARα, SREBP1 and ChREBP.[30–32] In this study, we initially found that in foam cells, liraglutide induced the expression of AMPKα1 and pho-AMPKα1, while inhibiting the expression of SREBP1 in a concentration-dependent manner. In addition, liraglutide-induced activation of AMPK/SREBP1 pathway is also dependent on GLP-1R.

A summary diagram that outlines the potential biochemical mechanisms of the action of liraglutide is shown in Figure 7. In foam cells, liraglutide inhibited oxidative stress and fatty degeneration, accompanied by the activation of the AMPK/SREBP1 pathway. As a limitation of this study, we only investigated the effect of liraglutide on the AMPK/SREBP1 pathway. Further studies are required to exclusively block the AMPK/SREBP1 pathway to elucidate whether this pathway mediates the effect of liraglutide on reducing oxidative stress and fatty degeneration.

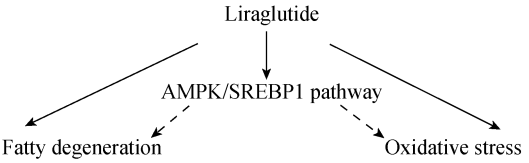

Figure 7. A diagram that outlines the potential biochemical mechanisms of the action of liraglutide. AMPK: AMP-activated protein kinase; SREBP1: sterol regulatory element binding transcription factor 1.

In conclusion, we demonstrated for the first time that liraglutide could affect the AMPK/SREBP1 pathway in oxLDL-stimulated Raw264.7 cells and this effect is dependent on GLP-1R. This study provided a potential molecular mechanism for the effect of liraglutide on reducing oxidative stress and fatty degeneration. It may help to improve the treatment of atherosclerotic vascular diseases.

Acknowledgement

This work was supported by the Science and Technology Plan Project of Hunan Province, P.R. China (2012SK3243). The authors declare no conflicts of interest.

References

1 Azen SP, Mack WJ, Cashin-Hemphill L, *et al.* Progression of coronary artery disease predicts clinical coronary events. Long-term follow-up from the Cholesterol Lowering Atherosclerosis Study. *Circulation* 1996; 93: 34–41.
2 Blankenhorn DH, Hodis HN. George Lyman Duff Memorial Lecture. Arterial imaging and atherosclerosis reversal. *Arterioscler Thromb* 1994; 14: 177–192.
3 Vigen C, Hodis HN, Selzer RH, *et al.* Relation of progression of coronary artery atherosclerosis to risk of cardiovascular events (from the Monitored Atherosclerosis Regression Study). *Am J Cardiol* 2005; 95: 1277–1282.
4 Wajcberg E, Amarah A. Liraglutide in the management of type 2 diabetes. *Drug Des Devel Ther* 2010; 4: 279–290.
5 Gaspari T, Welungoda I, Widdop RE, *et al.* The GLP-1 receptor agonist liraglutide inhibits progression of vascular disease via effects on atherogenesis, plaque stability and endothelial function in an ApoE(-/-) mouse model. *Diab Vasc Dis Res* 2013; 10: 353–360.
6 Ronnebaum SM, Patterson C, Schisler JC. Minireview: hey U(PS): metabolic and proteolytic homeostasis linked via AMPK and the ubiquitin proteasome system. *Mol Endocrinol* 2014; 28: 1602–1615.
7 Li D, Wang D, Wang Y, *et al.* Adenosine monophosphate-activated protein kinase induces cholesterol efflux from macrophage-derived foam cells and alleviates atherosclerosis in apolipoprotein E-deficient mice. *J Biol Chem* 2010; 285: 33499–33509.
8 Libby P, Geng YJ, Aikawa M, *et al.* Macrophages and atherosclerotic plaque stability. *Curr Opin Lipidol* 1996; 7: 330–335.
9 Vazquez G. TRPC channels as prospective targets in atherosclerosis: terra incognita. *Front Biosci (Schol Ed)* 2012; 4: 157–166.
10 Kataoka H, Kume N, Miyamoto S, *et al.* Expression of lectinlike oxidized low-density lipoprotein receptor-1 in human atherosclerotic lesions. *Circulation* 1999; 99: 3110–3117.
11 Miller YI, Choi SH, Fang L, *et al.* Lipoprotein modification and macrophage uptake: role of pathologic cholesterol transport in atherogenesis. *Subcell Biochem* 2010; 51: 229–251.
12 Endemann G, Stanton LW, Maden KS, *et al.* CD36 is a receptor for oxidized low density lipoprotein. *J Biol Chem* 1993; 268: 11811–11816.
13 Suzuki H, Kurihara Y, Takeya M, *et al.* A role for macrophage scavenger receptors in atherosclerosis and susceptibility to infection. *Nature* 1997; 386: 292–296.
14 Libby P. Inflammation in atherosclerosis. *Nature* 2002; 420: 868–874.
15 Steinberg D. Low density lipoprotein oxidation and its pathobiological significance. *J Biol Chem* 1997; 272: 20963–20966.
16 Tabas I, Williams KJ, Boren J. Subendothelial lipoprotein retention as the initiating process in atherosclerosis: update and therapeutic implications. *Circulation* 2007; 116: 1832–1844.
17 Greaves DR, Gordon S. Thematic review series: the immune system and atherogenesis. Recent insights into the biology of macrophage scavenger receptors. *J Lipid Res* 2005; 46: 11–20.
18 Schmitz G, Grandl M. Endolysosomal phospholipidosis and cytosolic lipid droplet storage and release in macrophages. *Biochim Biophys Acta* 2009; 1791: 524–539.
19 Yancey PG, Jerome WG. Lysosomal cholesterol derived from mildly oxidized low density lipoprotein is resistant to efflux. *J Lipid Res* 2001; 42: 317–327.
20 Yancey PG, Miles S, Schwegel J, *et al*. Uptake and trafficking of mildly oxidized LDL and acetylated LDL in THP-1 cells does not explain the differences in lysosomal metabolism of these two lipoproteins. *Microsc Microanal* 2002; 8: 81–93.
21 Dhaliwal BS, Steinbrecher UP. Cholesterol delivered to macrophages by oxidized low density lipoprotein is sequestered in lysosomes and fails to efflux normally. *J Lipid Res* 2000; 41: 1658–1665.
22 Itabe H. Oxidized low-density lipoproteins: what is understood and what remains to be clarified. *Biol Pharm Bull* 2003; 26: 1–9.
23 Zhou SW, Zhang M, Zhu M. Liraglutide reduces lipid accumulation in steatotic L-02 cells by enhancing autophagy. *Mol Med Rep* 2014; 10: 2351–2357.
24 Gao H, Xu L, Li D, *et al*. Effects of glucagon-like peptide-1 on liver oxidative stress, TNF-α and TGF-β1 in rats with non-alcoholic fatty liver disease. *Nan Fang Yi Ke Da Xue Xue Bao* 2013; 33: 1661–1664 (In Chinese).
25 Zampetaki A, Dudek K, Mayr M. Oxidative stress in atherosclerosis: the role of microRNAs in arterial remodeling. *Free Radic Biol Med* 2013; 64: 69–77.
26 Hardie DG. The AMP-activated protein kinase pathway-new players upstream and downstream. *J Cell Sci* 2004; 117: 5479–5487.
27 Cheung PC, Salt IP, Davies SP, *et al.* Characterization of AMP-activated protein kinase gamma-subunit isoforms and their role in AMP binding. *Biochem J* 2000; 346: 659–669.
28 Hardie DG. AMP-activated protein kinase: a master switch in glucose and lipid metabolism. *Rev Endocr Metab Disord* 2004; 5: 119–125.
29 Hardie DG, Pan DA. Regulation of fatty acid synthesis and oxidation by the AMP-activated protein kinase. *Biochem Soc Trans* 2002; 30: 1064–1070.
30 Bronner M, Hertz R, Bar-Tana J. Kinase-independent transcriptional co-activation of peroxisome proliferator-activated receptor alpha by AMP-activated protein kinase. *Biochem J* 2004; 384: 295–305.
31 Li Y, Xu S, Mihaylova MM, *et al.* AMPK phosphorylates and inhibits SREBP activity to attenuate hepatic steatosis and atherosclerosis in diet-induced insulin-resistant mice. *Cell Metabolism* 2011; 13: 376–388.
32 Kawaguchi T, Osatomi K, Yamashita H, *et al.* Mechanism for fatty acid "sparing" effect on glucose-induced transcription: regulation of carbohydrate-responsive element-binding protein by AMP-activated protein kinase. *J Biol Chem* 2000; 277: 3829–3835.